

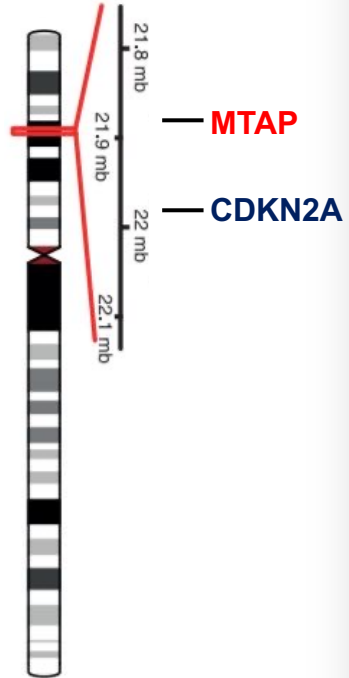


*MTA-cooperative PRMT5
Inhibitors for the Treatment of
MTAP-deleted Cancers*

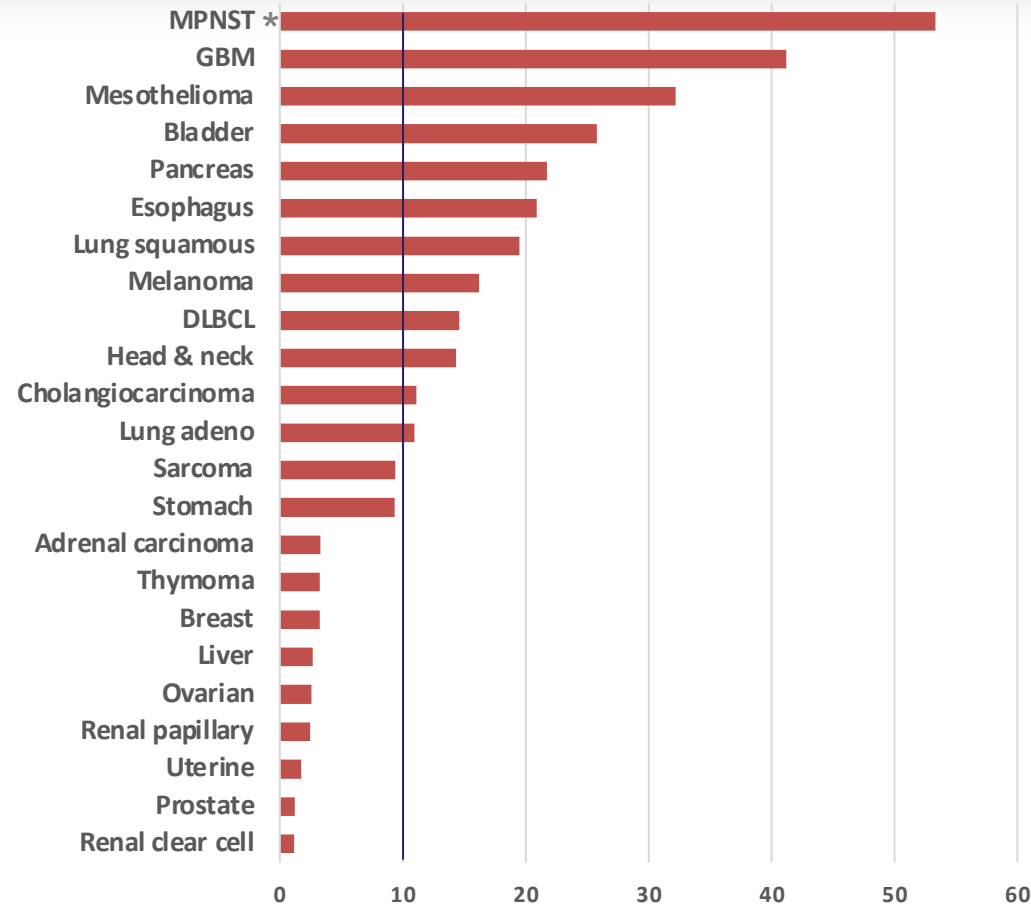
Kevin Cottrell
Applied Pharmaceutical Chemistry 2024
April 4, 2024

PRMT5 provides a large opportunity for treatment of cancer

Chromosome 9



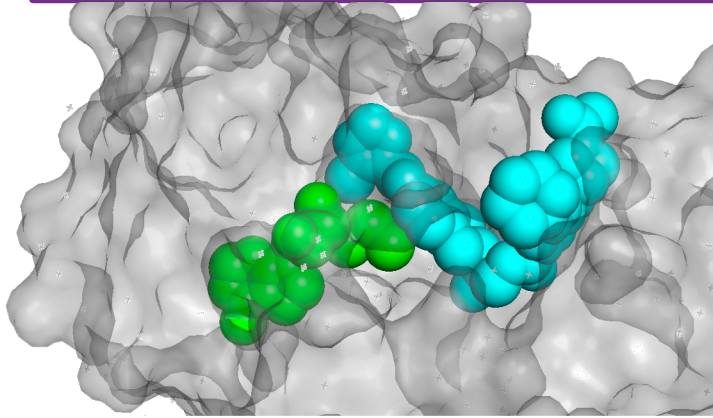
MTAP homozygous deletion frequency



10-15% of all human cancers are MTAP-deleted

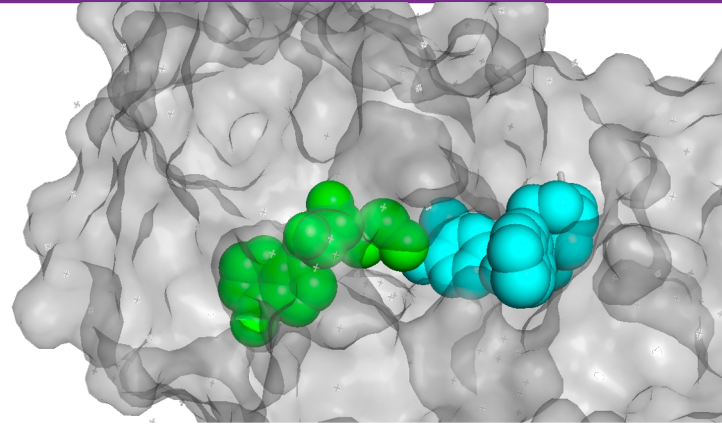
- MTAP is co-deleted with CDKN2A
- Clear path to clinical POC in MTAP-null solid tumors
- Potential for histology-agnostic registration

Tango MTA cooperative PRMT5 inhibitors



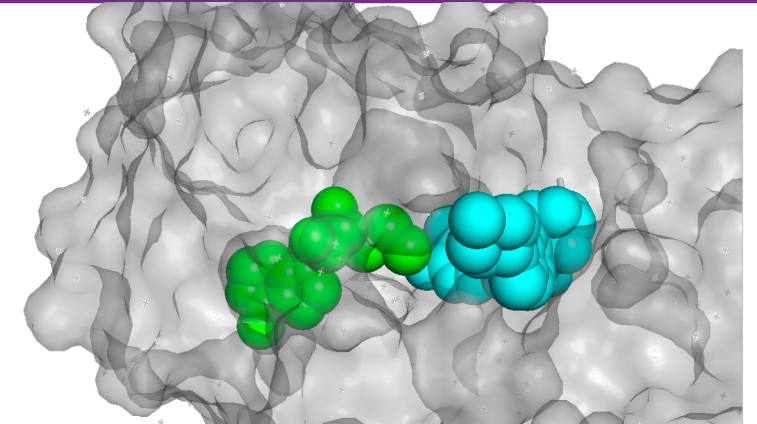
Rational Design

- SBDD from known starting points
- First reported MTA-cooperative PRMT5 inhibitors
- US11077101B1, WO2021086879
- Poster at 2024 NMCS (Seattle) and manuscript in progress



TNG908

- HTS starting point
- Brain penetrant, potentially active in GBM patients
- Currently in Phase 1/2 clinical trial (NCT05275478)
- Manuscript publishing this week

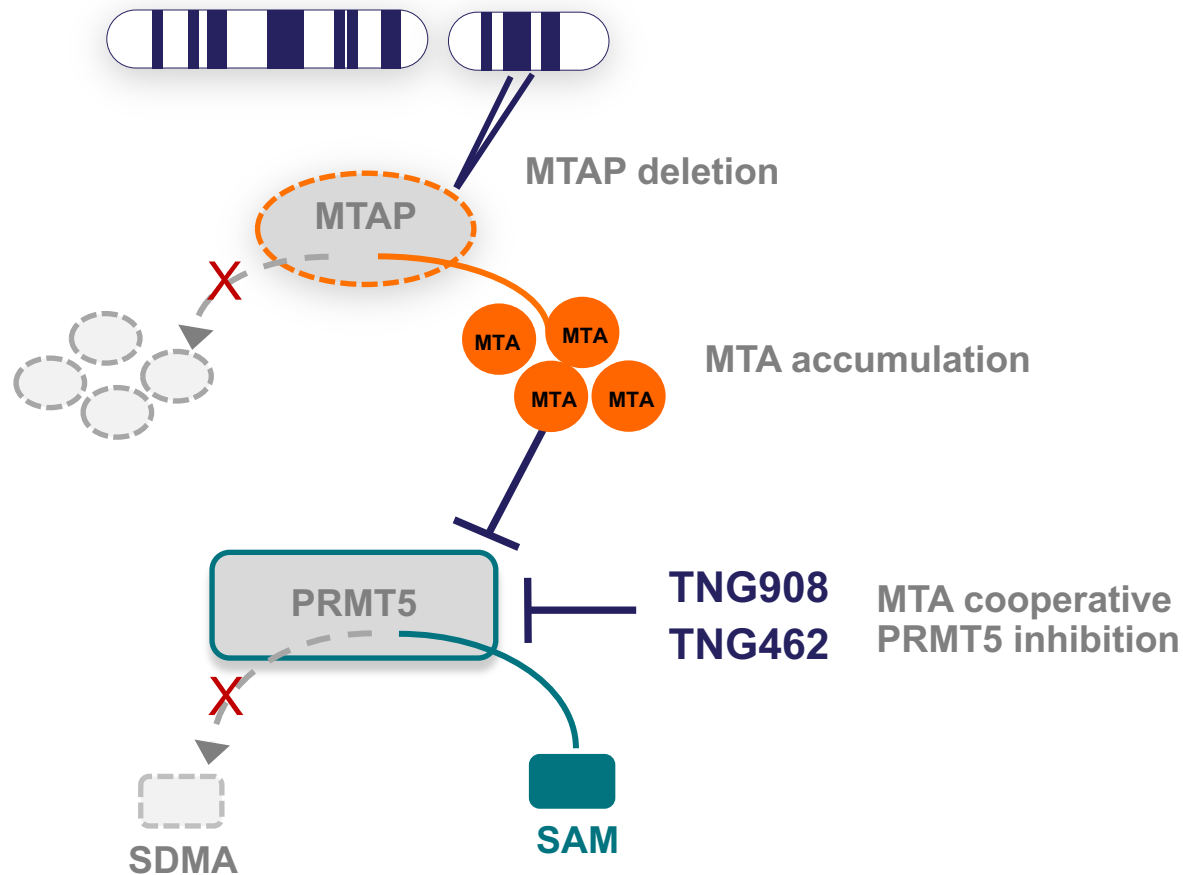


TNG462

- Next gen program
- ~30x more potent than TNG908 with increased selectivity
- Currently in Phase 1/2 clinical trial (NCT05732831)
- Structure disclosed at ACS Nat'l Mtg (San Francisco) 2023, manuscript in progress

PRMT5 and MTAP are a synthetic lethal pair

Cancers with MTAP deletion are more vulnerable to PRMT5 inhibition than normal cells

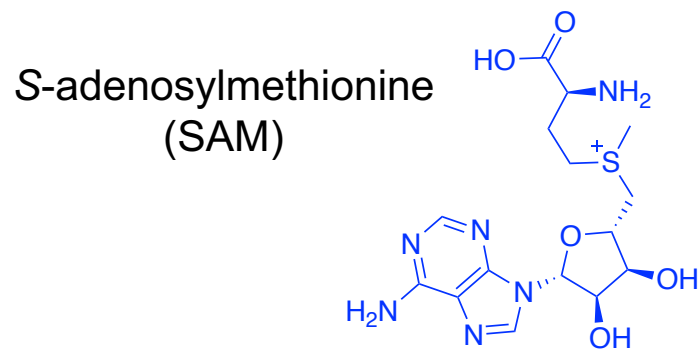


Mechanism of action

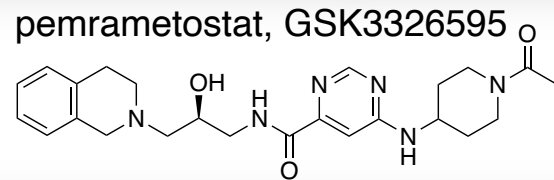
- MTAP deletion causes MTA to accumulate
- MTA binds to and inhibits PRMT5
- MTA-cooperative PRMT5 inhibitors selectively bind to the PRMT5-MTA complex and selectively kill MTAP-deleted cancer cells

Mavrakis et al., Science 2016; Kryukov et al., Science 2016; Marjon et al., Cell Reports 2016

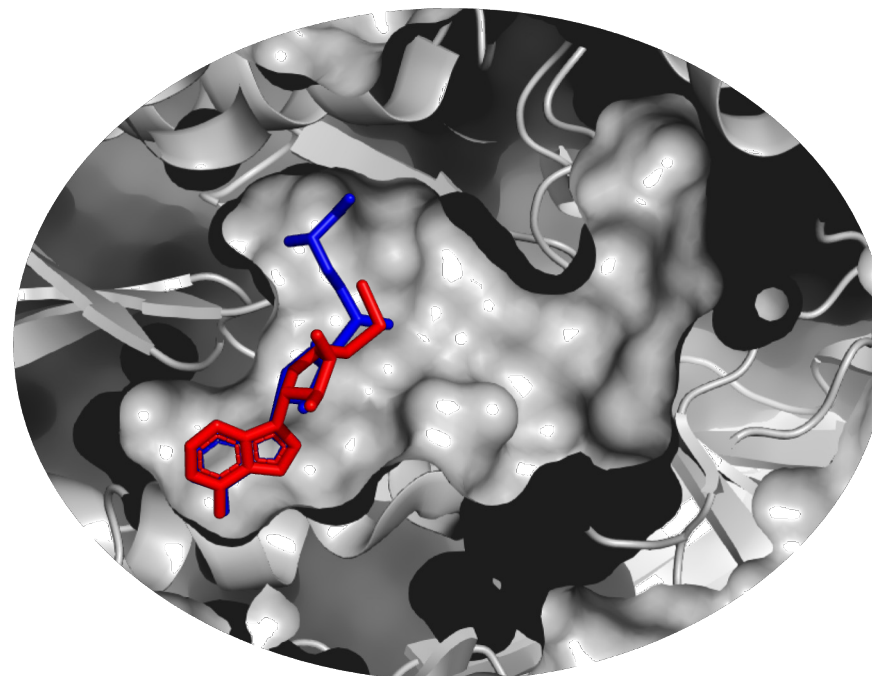
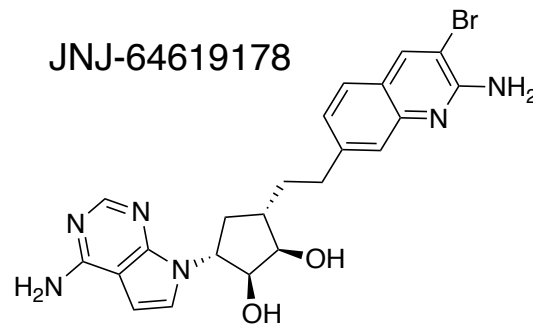
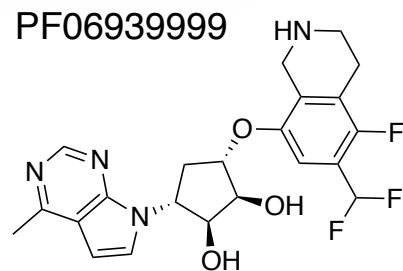
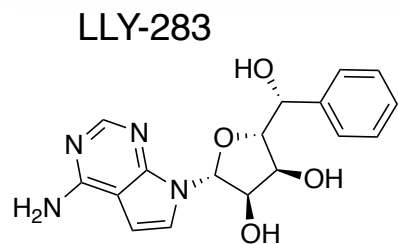
Multiple mechanisms of inhibition available for PRMT5



SAM uncompetitive

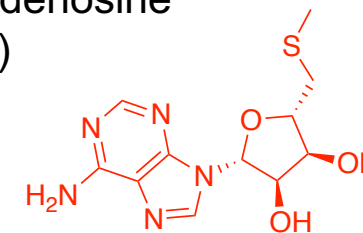


SAM competitive

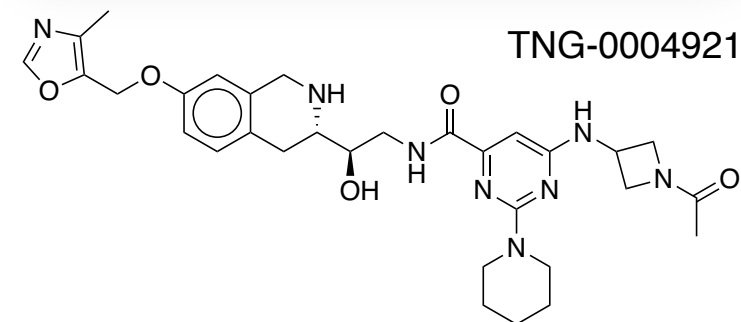


PRMT5 cofactor and substrate binding sites

5'-methylthioadenosine (MTA)



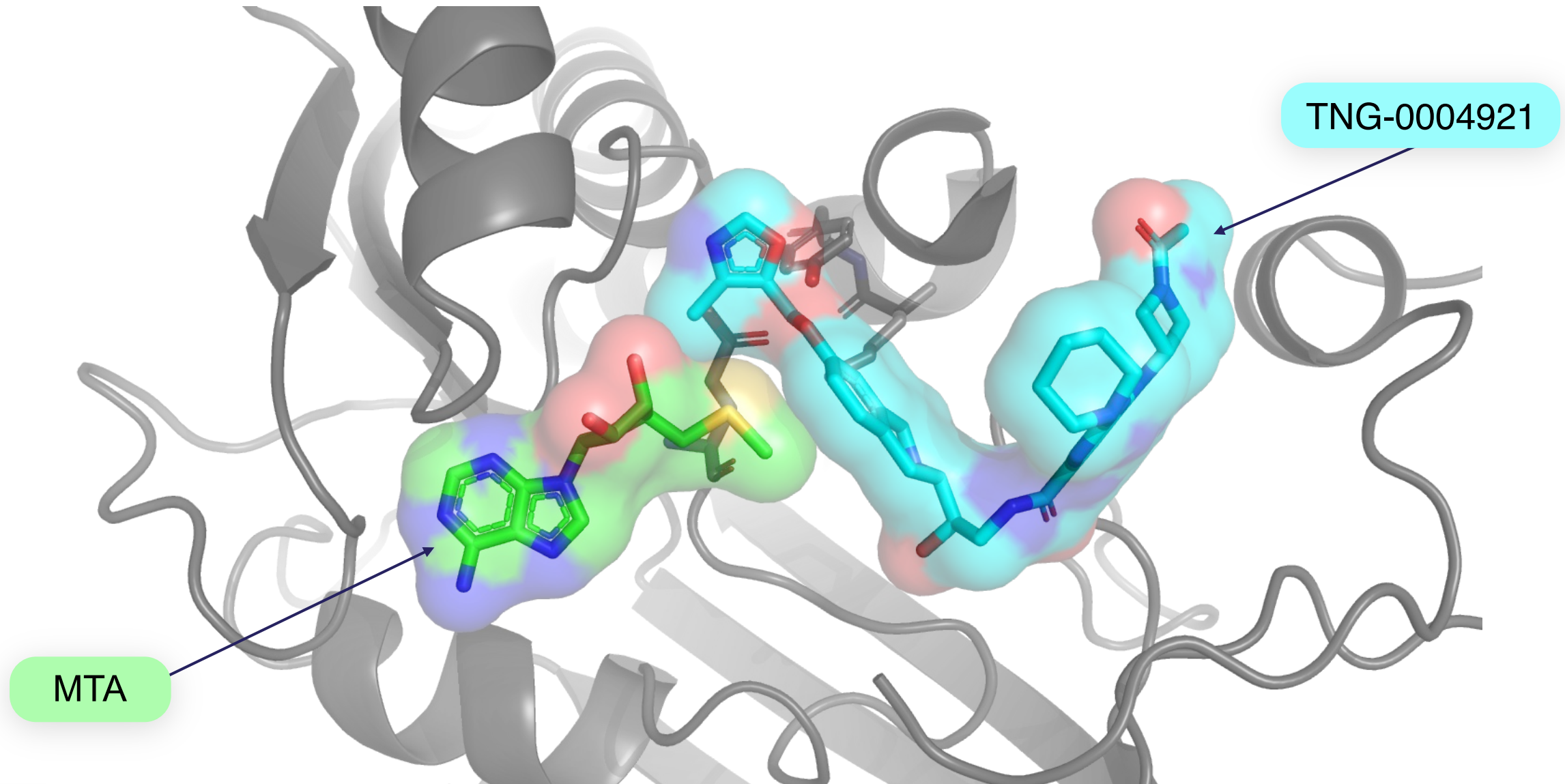
MTA uncompetitive



	MTAP del	MTAP WT
Cellular biomarker IC ₅₀ (μM)	0.093	4.37
Cellular viability GI ₅₀ (μM)	3.48	> 20

WO2021086879 (6 May 2021)

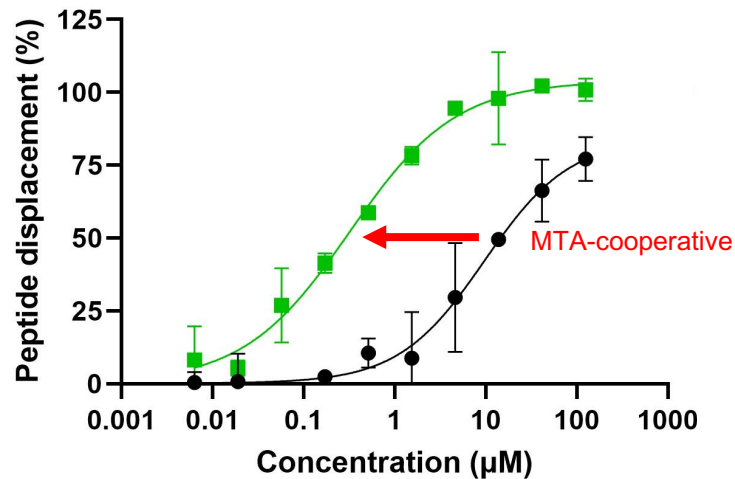
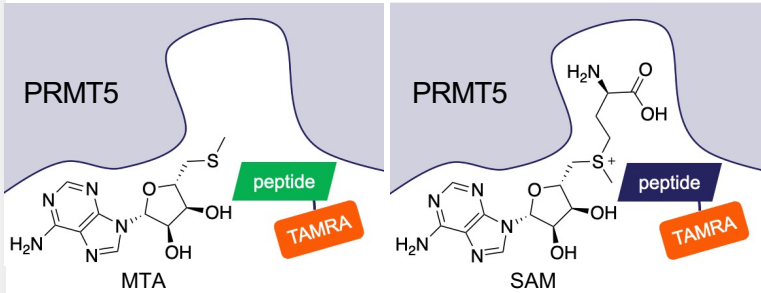
Crystal structure of first reported MTA-cooperative inhibitor series in PRMT5•MTA complex



Assays to measure biochemical and cellular selectivity

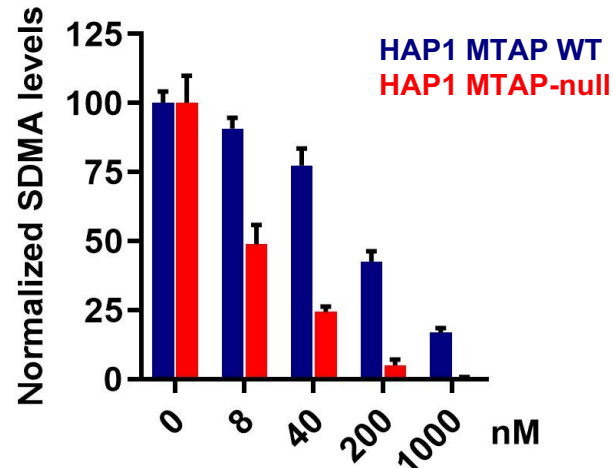
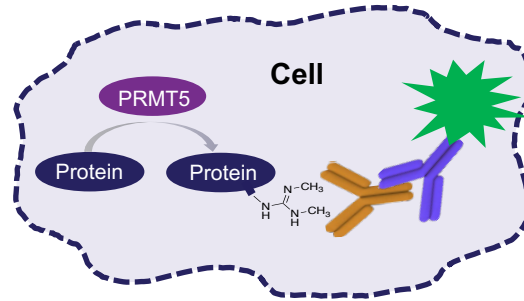
Biochemical

Fluorescence polarization displacement of TAMRA-labeled peptide



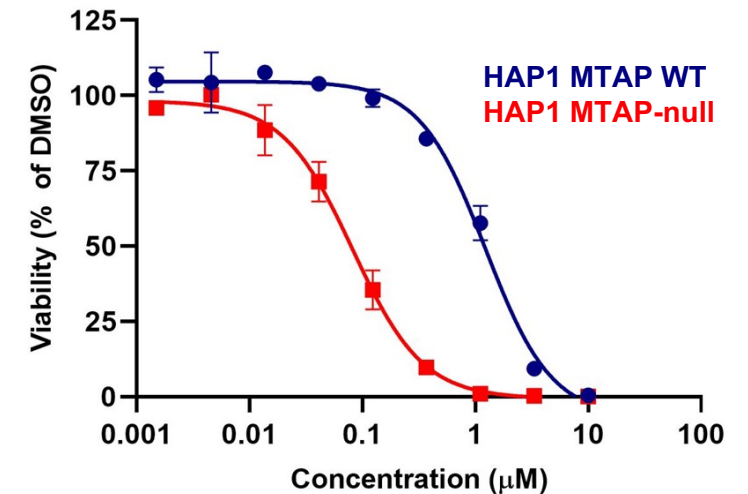
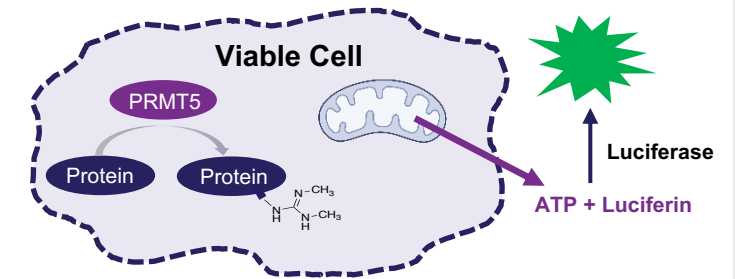
Cellular PD

In-Cell Western detection of SDMA (symmetric dimethylarginine) in HAP1 MTAP isogenic cell lines

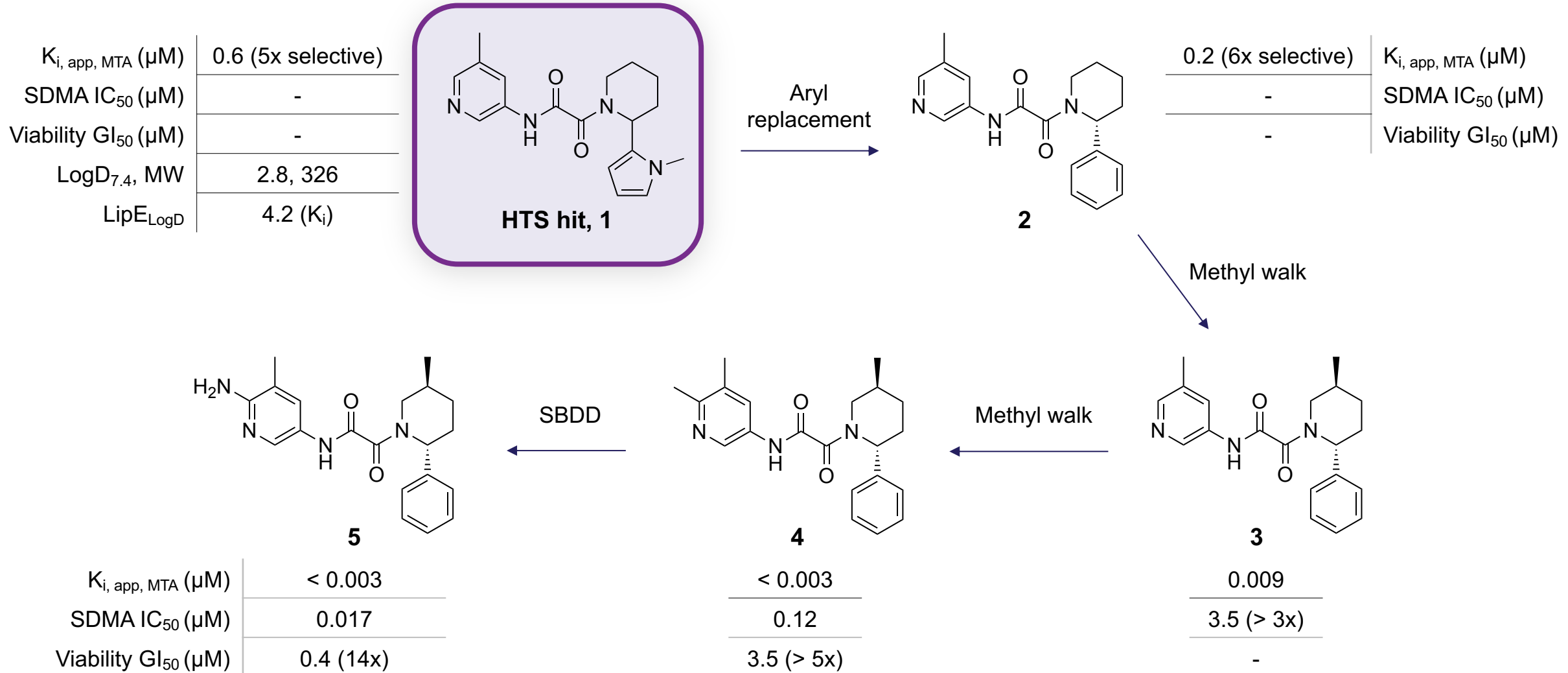


Cellular viability

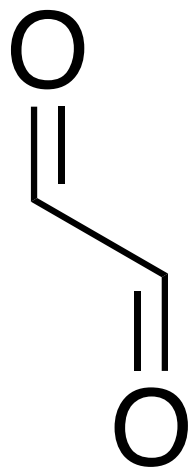
7-day viability assay assessed by CellTiter-Glo in HAP1 MTAP-isogenic cell lines



Evolution of biochemical HTS hit toward clinical candidate TNG908



1,2-dicarbonyl is widely considered a structural alert

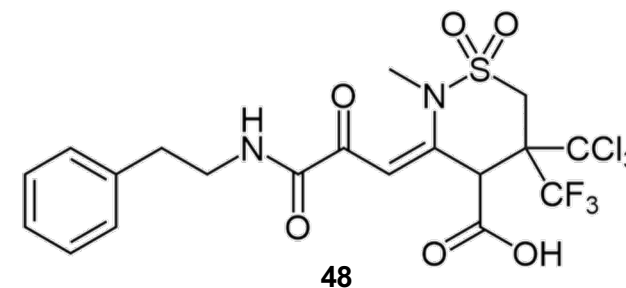


alpha dicarbonyl
C(=O)!@C(=O)

2011: “1,2-dicarbonyl: metabolically unstable/potential toxicity due to mutagenicity”

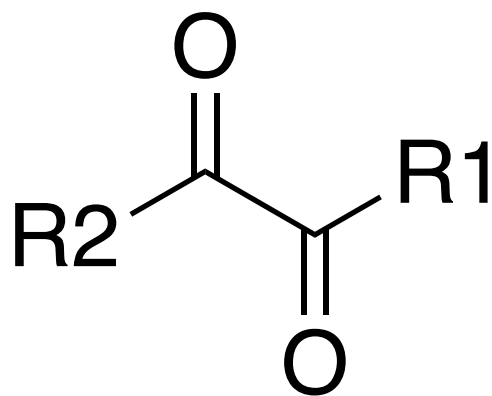
2016: “Trifluoromethyl ketone, aldehyde, and alpha_dicarbonyl FG filters show higher levels of promiscuity but are at the lower end of the high ranking”

2023: “Moreover, multiple structures seemed potentially toxic (e.g., ...**48** contains a potentially mutagenic 1,2-dicarbonyl group)”



(a) Pearce, B. C.; Sofia, M. J.; Good, A. C.; Drexler, D. M.; Stock, D. A. An Empirical Process for the Design of High-Throughput Screening Deck Filters. *J. Chem. Inf. Model.*, **2016**, 46, 1060-1068. (b) Huggins, D. J.; Venkitaraman, A. R.; and Spring, D. R. Rational Methods for the Selection of Diverse Screening Compounds. *ACS Chem. Biol.*, **2011**, 6, 3, 208-217. (c) Rishton, G. M.; Reactive Compounds and in vitro False Positives in HTS. *Drug Discovery Today*. **1997**, 2, 9, 382-384. (d) Ivanenkov, Y.; Zagribelnyy, B.; Malyshev, A.; Evteev, S.; Terentiev, V.; Kamyra, P.; Bezrukov, D.; Aliper, A.; Ren, F.; Zhavoronkov, A. The Hitchhiker's Guide to Deep Learning Driven Generative Chemistry. *ACS MedChem Lett.*, **2023**, 14, 901-915.

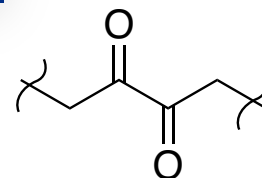
“Dicarbonyl” is generally associated with reactivity



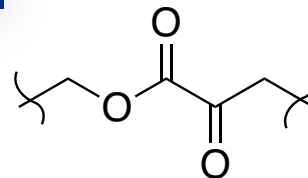
R1 = C; R2 = C, O

R1 = N; R2 = O

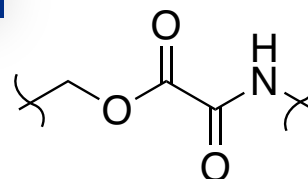
α,β -diketone



α -ketoester

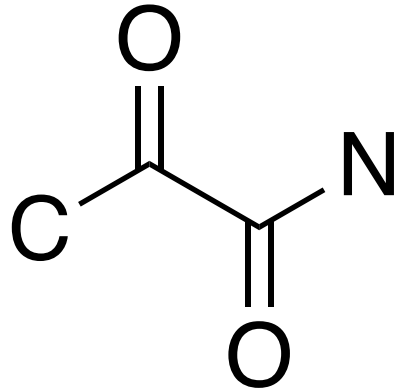


oxamate



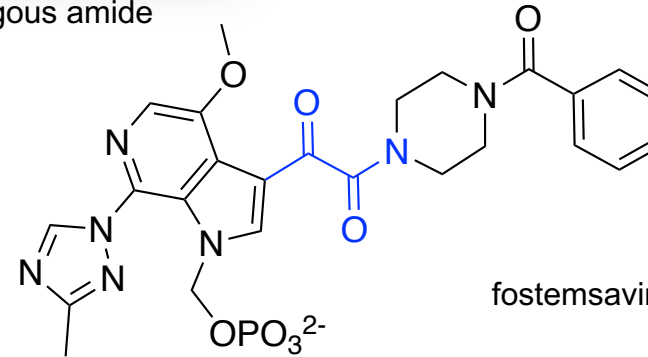
- Reactive
- Subject to hydrolysis
- Generally not found in medchem literature
- Frequent building blocks for chemical synthesis

α -ketoamides are well-precedented, both direct and vinylogous



glyoxamide

Vinylogous amide

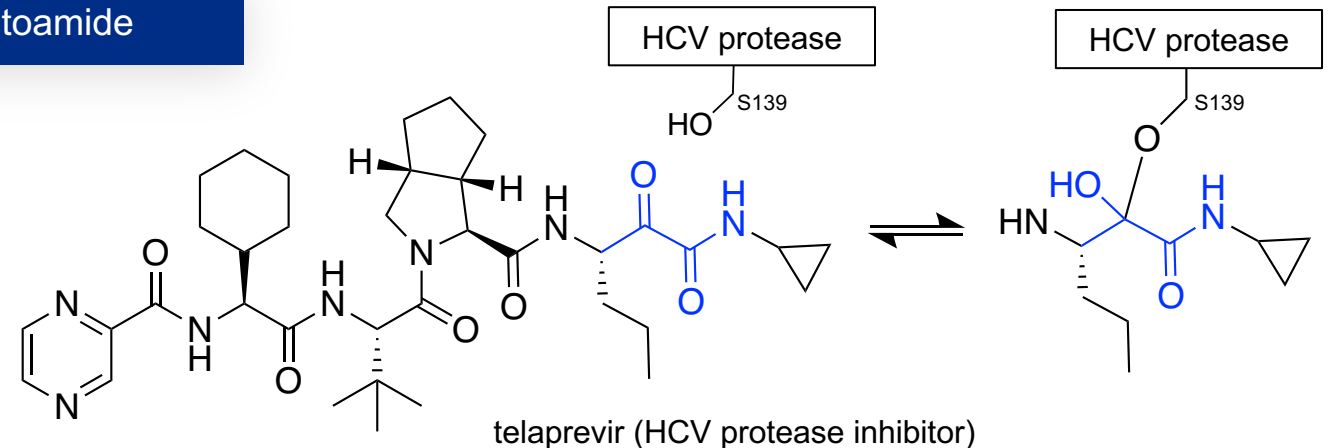


fostemsavir (HIV-1 attachment inhibitor)

α -ketoamide

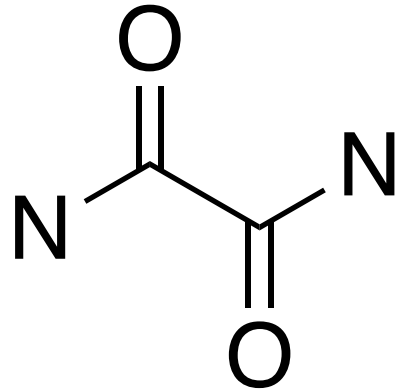
Hallmarks of reactivity and metabolic stability

- Nucleophilic attack, hydrate, epimerization
- Phase 1 reductions including via MDR, SDR, AKR, QR

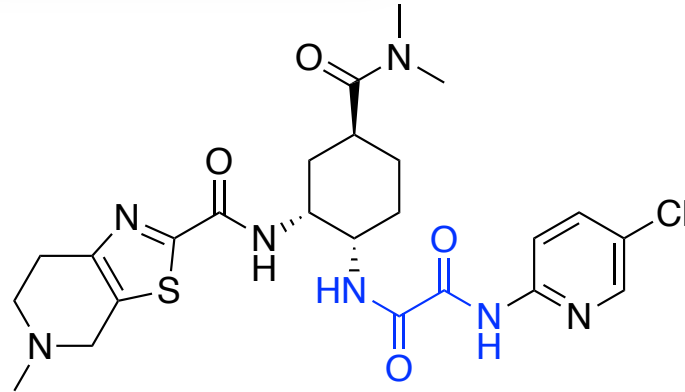


telaprevir (HCV protease inhibitor)

Oxamides are less common, but have strong precedent



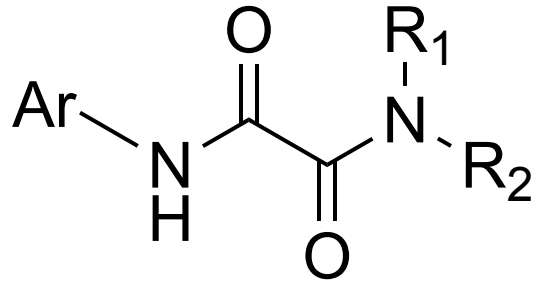
oxamide



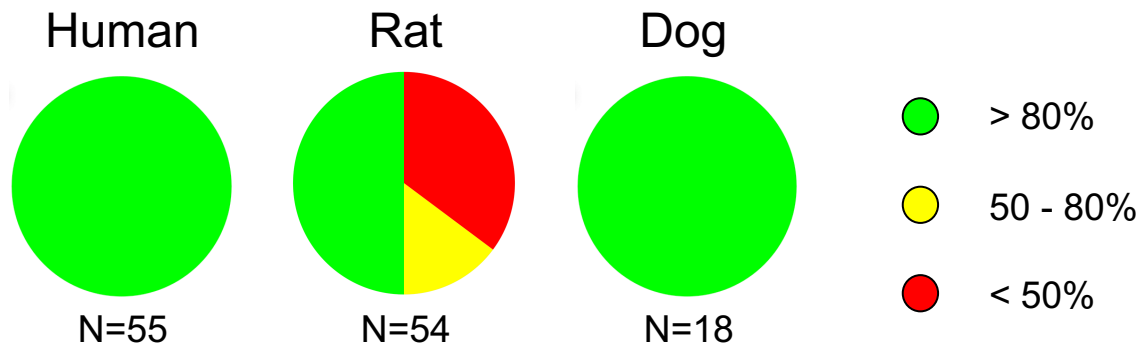
- Edoxaban (Lixiana)
- Factor Xa inhibitor
- US approval 2015
- ~\$1.5B sales, 2022

- Chemically unreactive in biorelevant setting
- Not electrophilic
- Stable in biological media
- Viable substructure for medicinal chemistry optimization

Compound stability dependent on medium and species

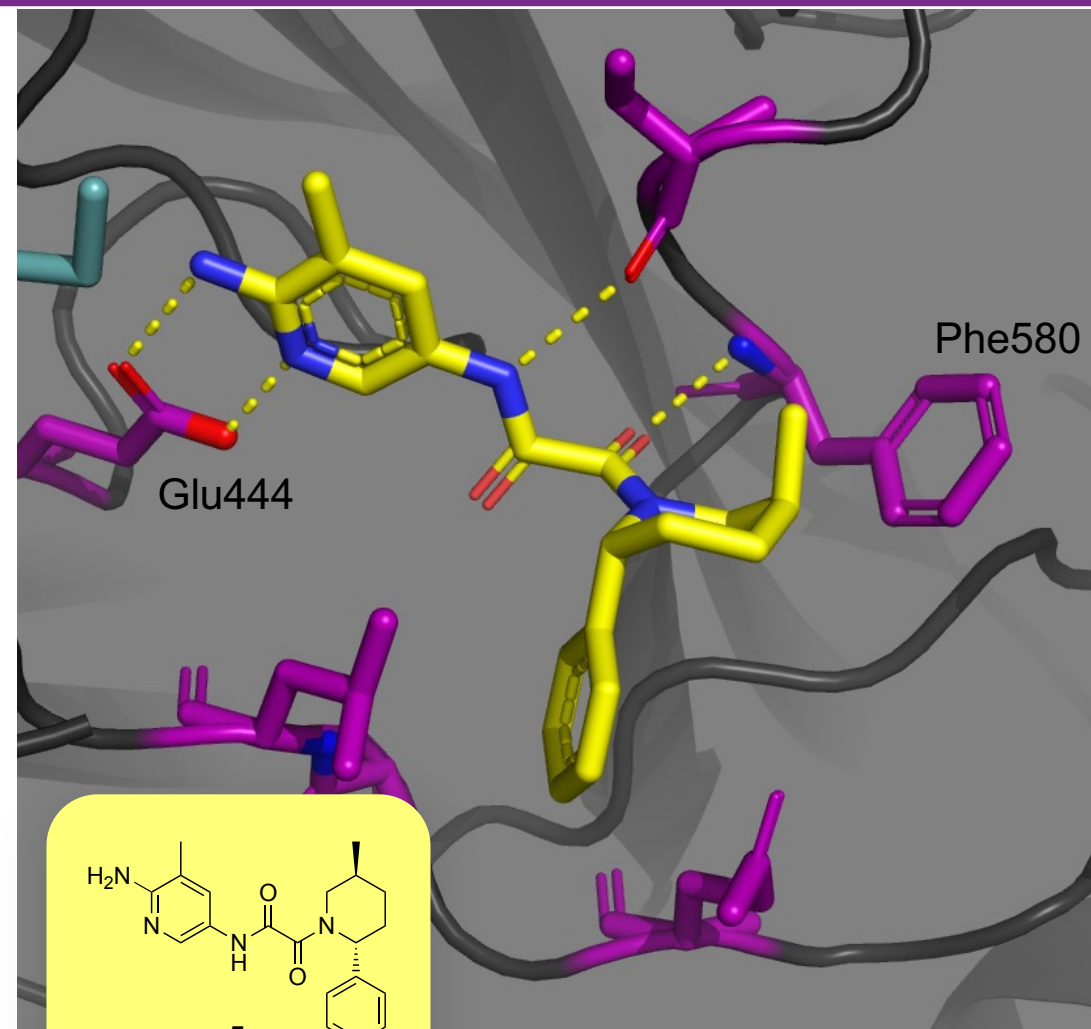
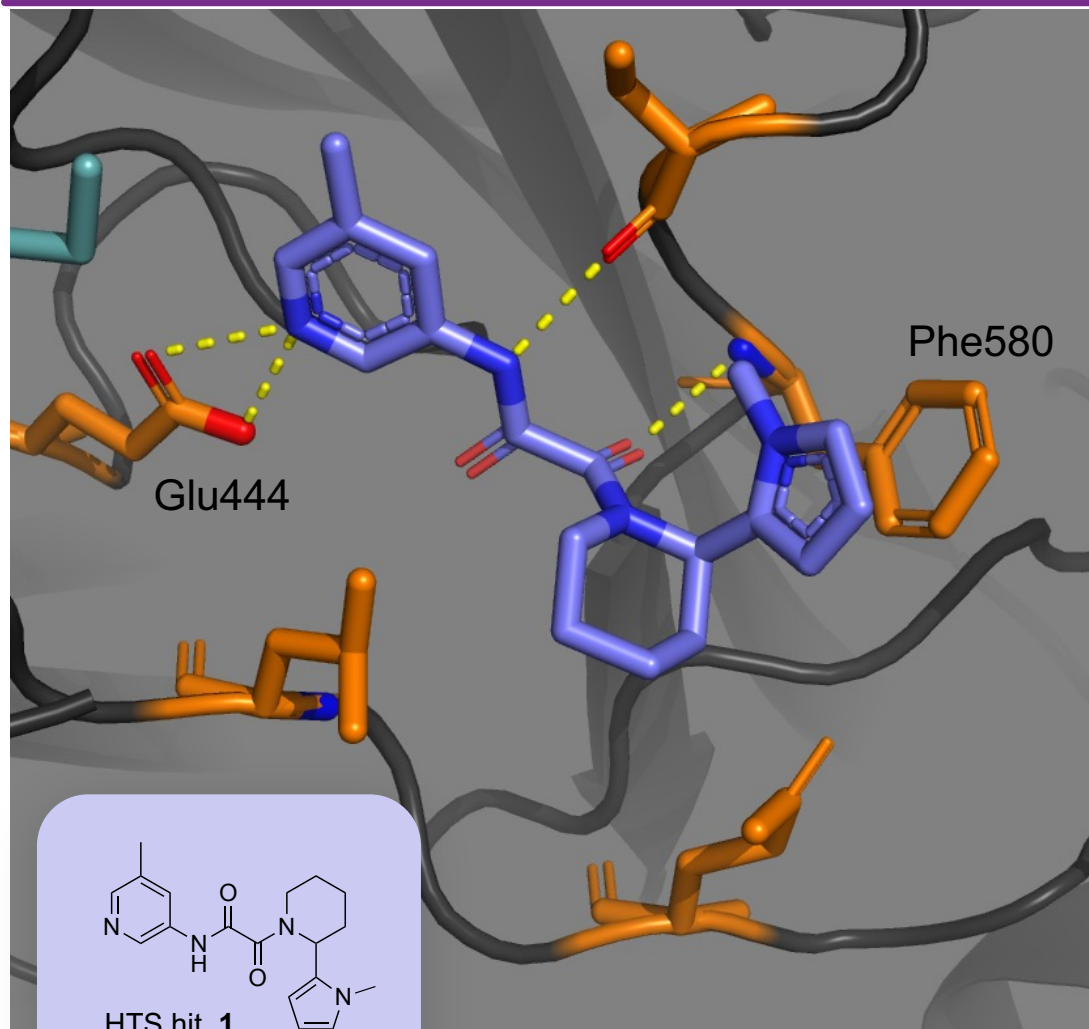


Plasma stability @ 2h

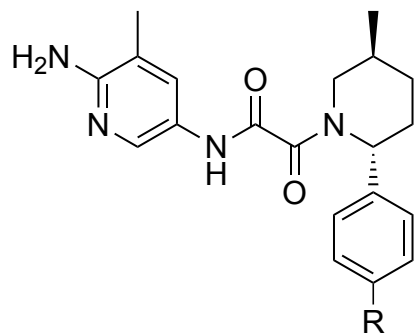


- Stable in buffer pH 1-13
- Plasma: Stable in dog and human, variable in rodent
- Limited utility of rat *in vivo* data
 - Poor *in vivo* in rat
 - Plasma stability
 - Renal clearance
- Drove early program with HLM
- Utilized higher species PK when possible

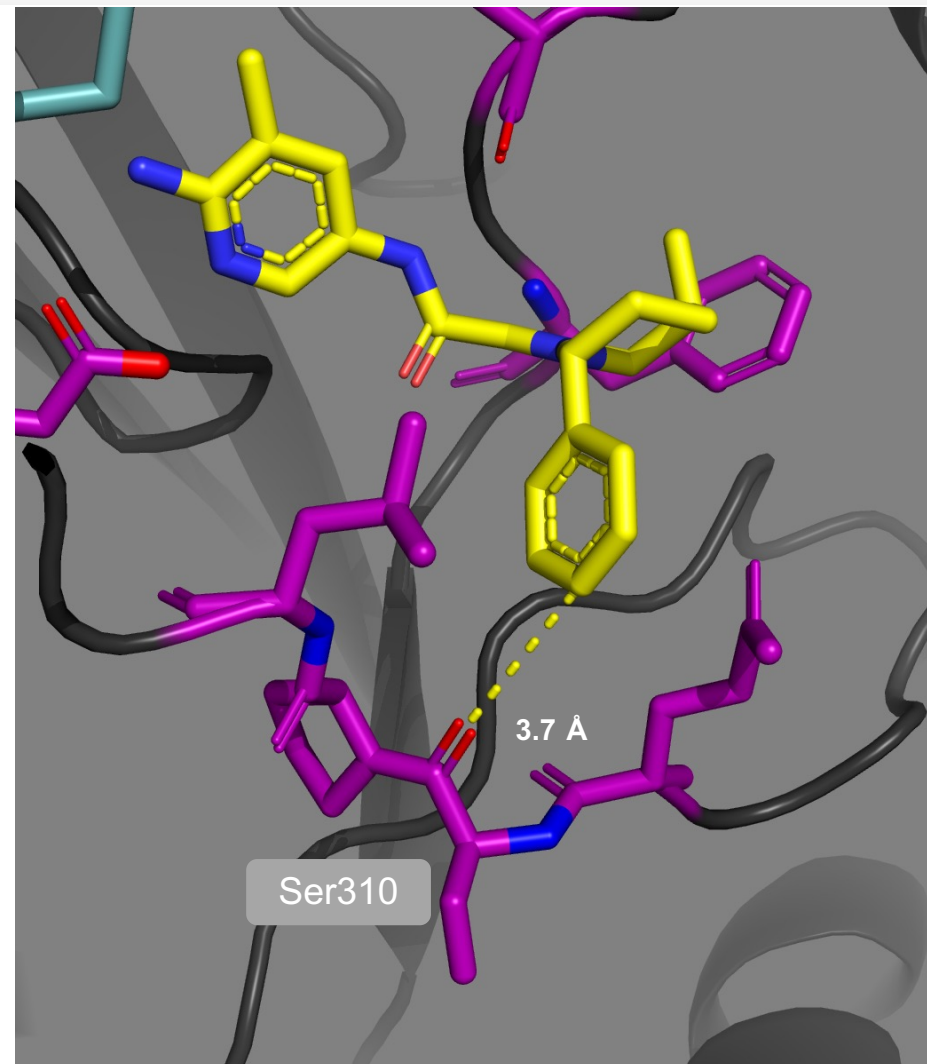
Always confirm your assumptions throughout the program



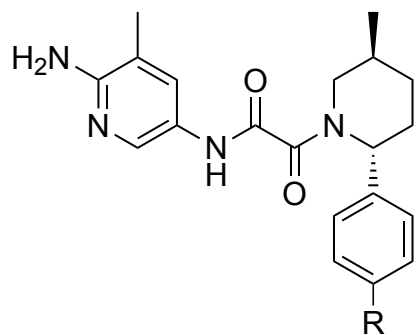
Hypothesis: H-bond with Ser310 C=O could improve potency



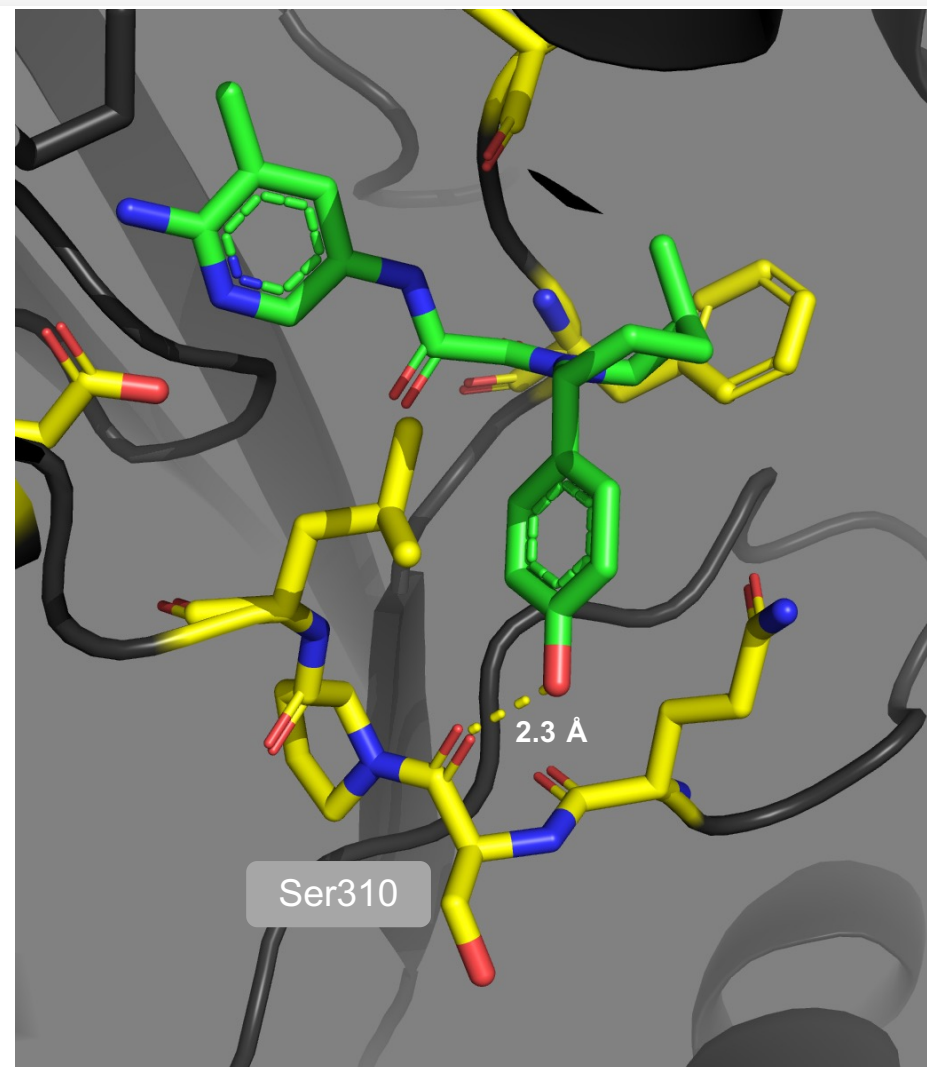
R	H
Viability GI ₅₀ (μM)	0.4
Selectivity to WT	14x



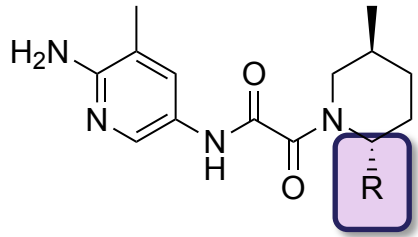
H-bond with Ser310 C=O improves potency 7-fold



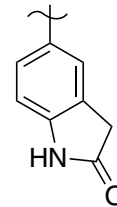
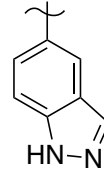
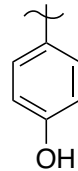
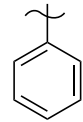
R	H	OH
Viability GI ₅₀ (μM)	0.4	0.06
Selectivity to WT	14x	23x



NH containing phenol isosteres lack properties amenable for BBB penetrance

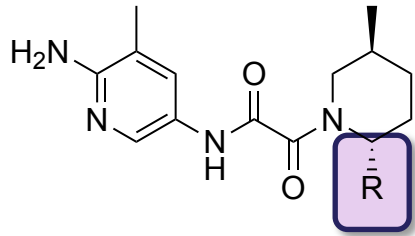


- Many phenol isosteres retain potency
- Addition of NH HBD reduces permeability and increases efflux

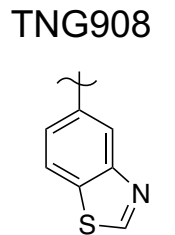
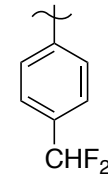
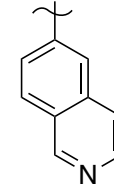
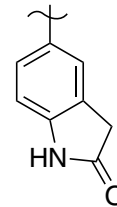
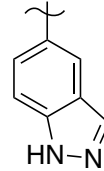
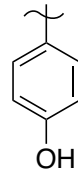
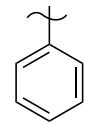


Viability GI ₅₀ (μM)	0.4	0.06	0.05	0.06
Selectivity (to GI ₅₀ , WT)	14	23	21	20
MDCK A-B (x10 ⁶ cm/s)	11	6	5	1
Mdr1 efflux ratio	1	10	18	34

Benzothiazole replacement of phenol retains potency and properties, yielding brain penetrant TNG908



- Many phenol isosteres retain potency
- Addition of NH HBD reduces permeability and increases efflux
- Use of S-carbonyl interaction provides balance of potency and properties



	0.4	0.06	0.05	0.06	0.2	0.9	TNG908 0.1
Viability GI ₅₀ (μM)	0.4	0.06	0.05	0.06	0.2	0.9	0.1
Selectivity (to GI ₅₀ , WT)	14	23	21	20	12	3	15
MDCK A-B (x10 ⁶ cm/s)	11	6	5	1	18	14	16
Mdr1 efflux ratio	1	10	18	34	1	0.6	3

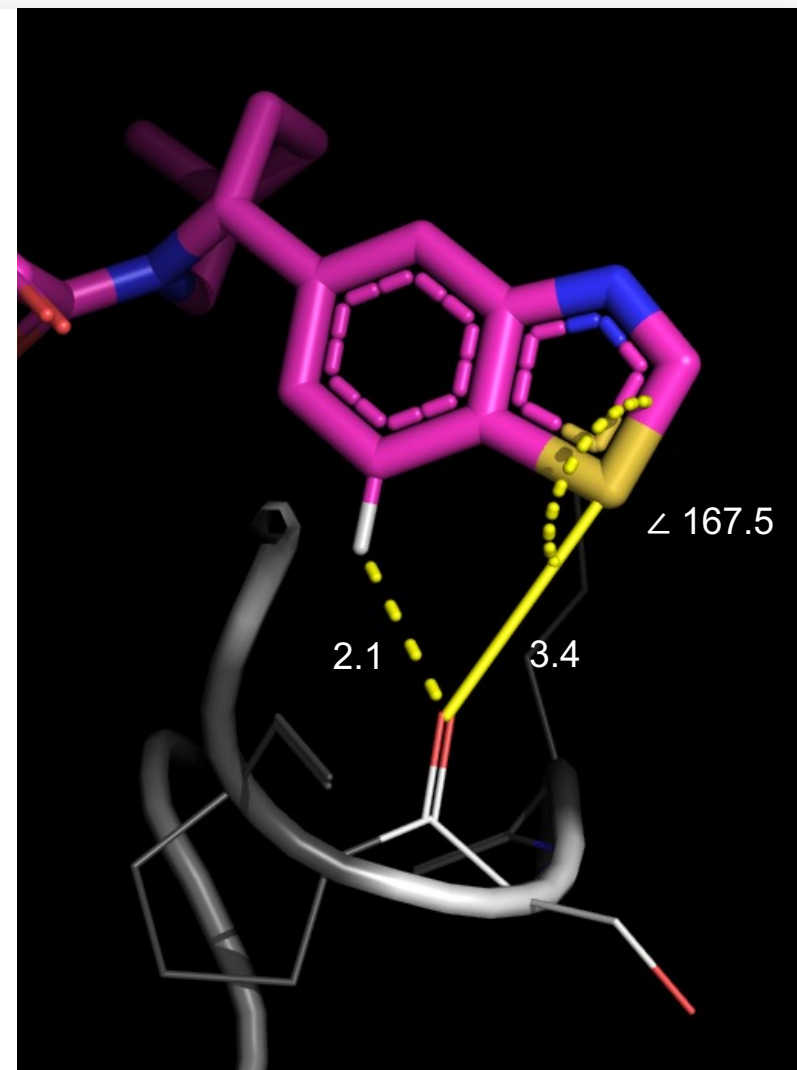
Use of sulfur is key for property / potency balance

Key interactions within acceptable ranges

- Bidentate carbonyl contact with S and H_{Ar}
- S···O=C, 3.4 Å (C-S σ* orbital)
- H···O=C, 2.1 Å
- 167° dihedral angle (S-O-C)

Important and underutilized interaction

Gain ligand-protein contact without increased HBD



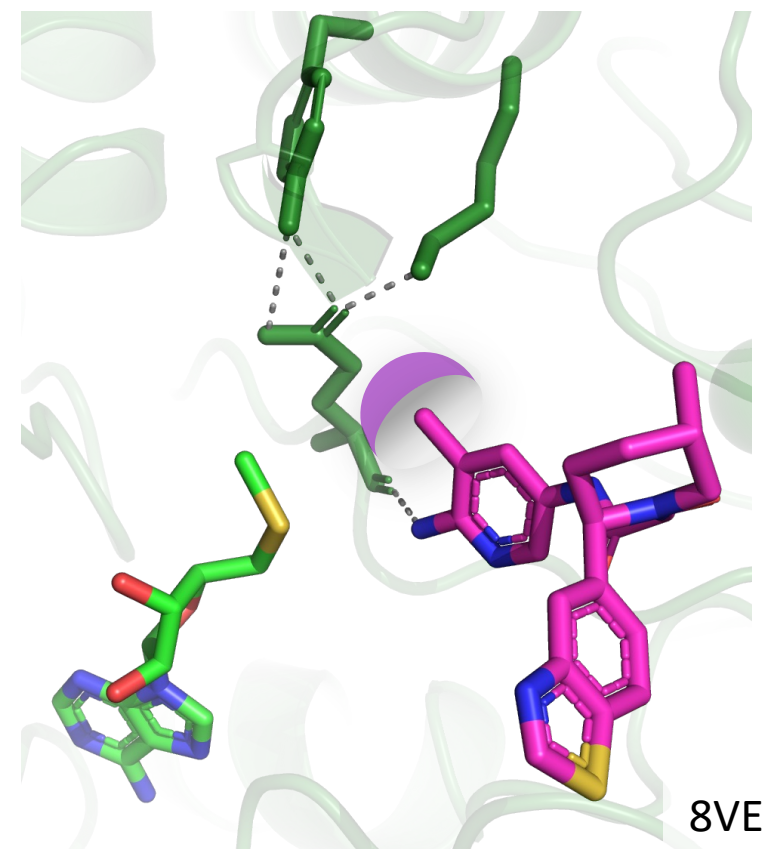
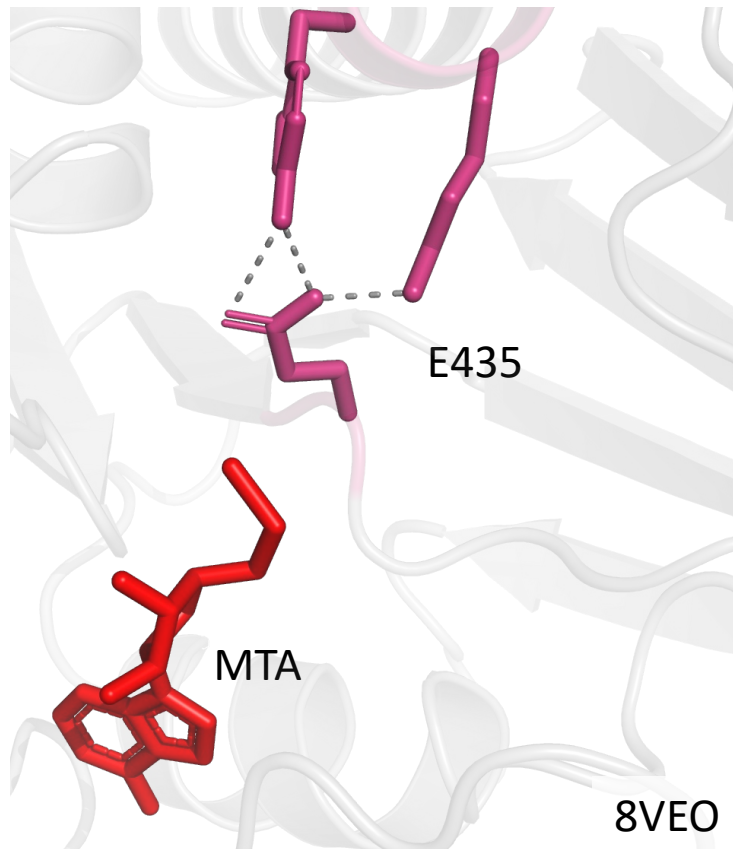
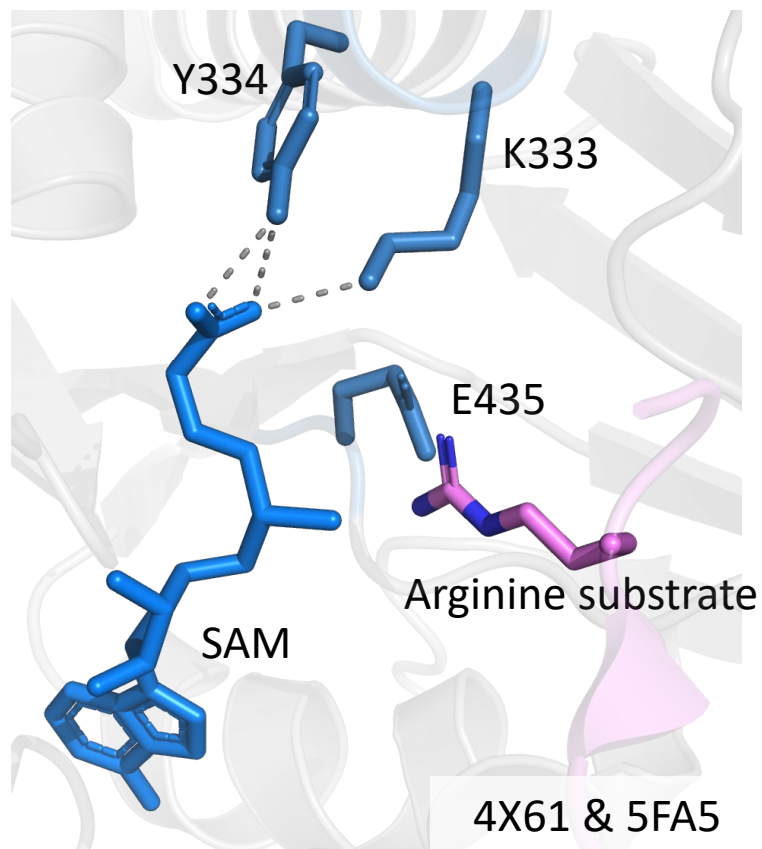
(a) Beno, B. R.; Yeung, K.-S.; Bartberger, M. D.; Pennington, L. D.; Meanwell, N. A. A Survey of the Role of Noncovalent Sulfur Interactions in Drug Design. *J Med Chem* **2015**, *58* (11), 4383–4438. <https://doi.org/10.1021/jm501853m>.
(b) Koebel, M. R.; Cooper, A.; Schmadeke, G.; Jeon, S.; Narayan, M.; Sirimulla, S. S···O and S···N Sulfur Bonding Interactions in Protein–Ligand Complexes: Empirical Considerations and Scoring Function. *J. Chem. Inf. Model.* **2016**, *56* (12), 2298–2309. <https://doi.org/10.1021/acs.jcim.6b00236>.
(c) Zhang, X.; Gong, Z.; Li, J.; Lu, T. Intermolecular Sulfur···Oxygen Interactions: Theoretical and Statistical Investigations. *J. Chem. Inf. Model.* **2015**, *55* (10), 2138–2153. <https://doi.org/10.1021/acs.jcim.5b00177>.

Glutamate 435 rotamer-lock is key to selective binding with MTA

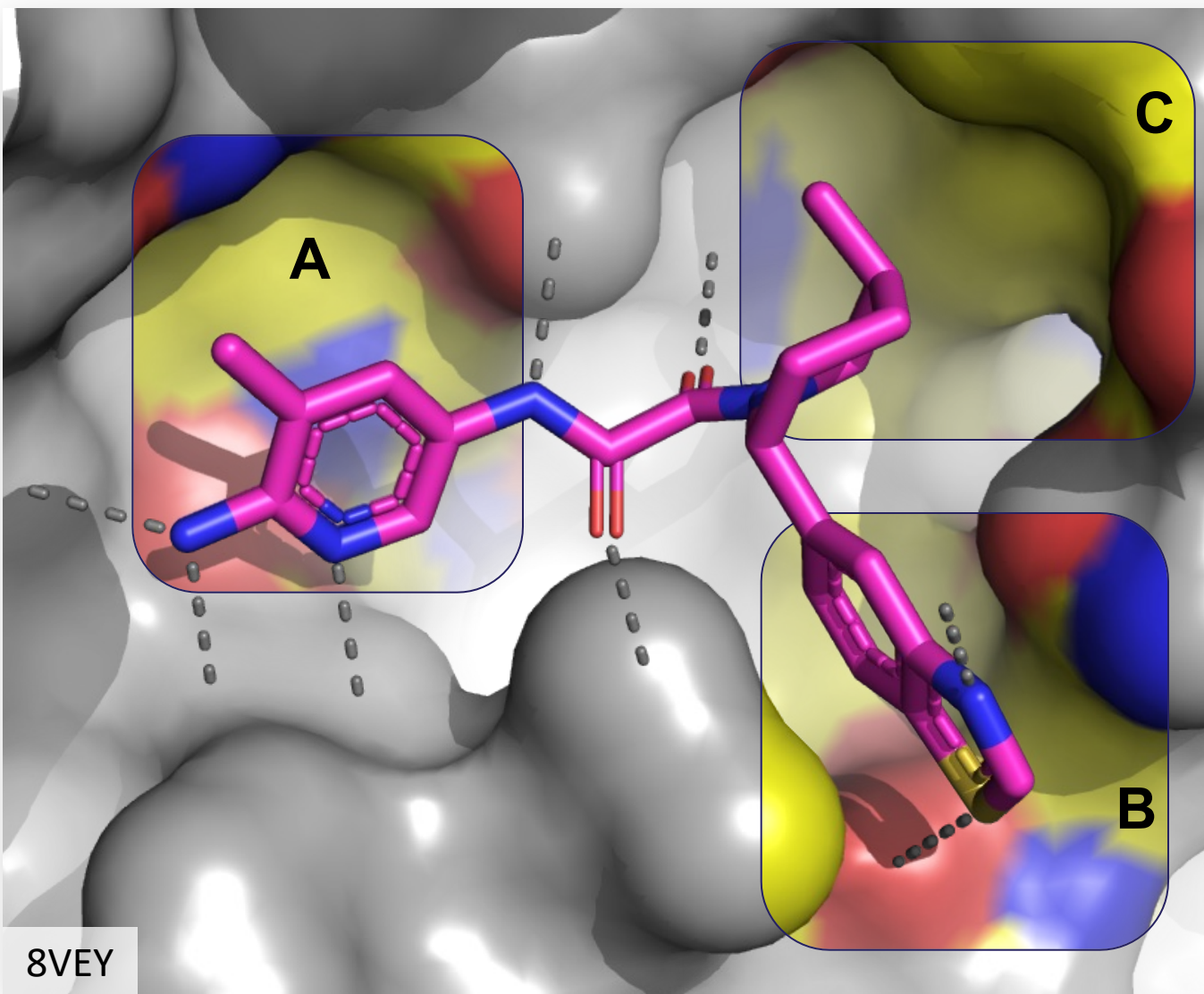
- SAM engages Y334/K333 in bioactive state
- E435 folded behind substrate

- E435 engages Y334/K333 sidechain when MTA is bound

- TNG908 engages E435 backbone C=O and sterically locks rotamer



TNG908 binding analysis suggests areas for further exploration



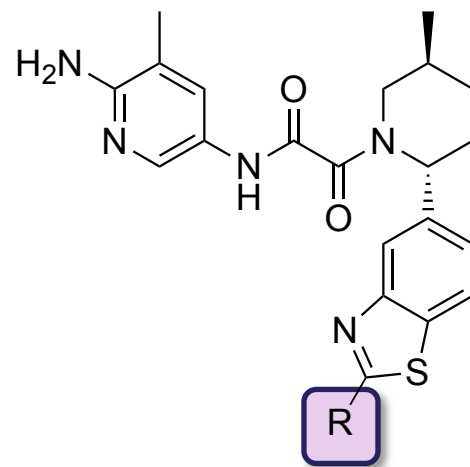
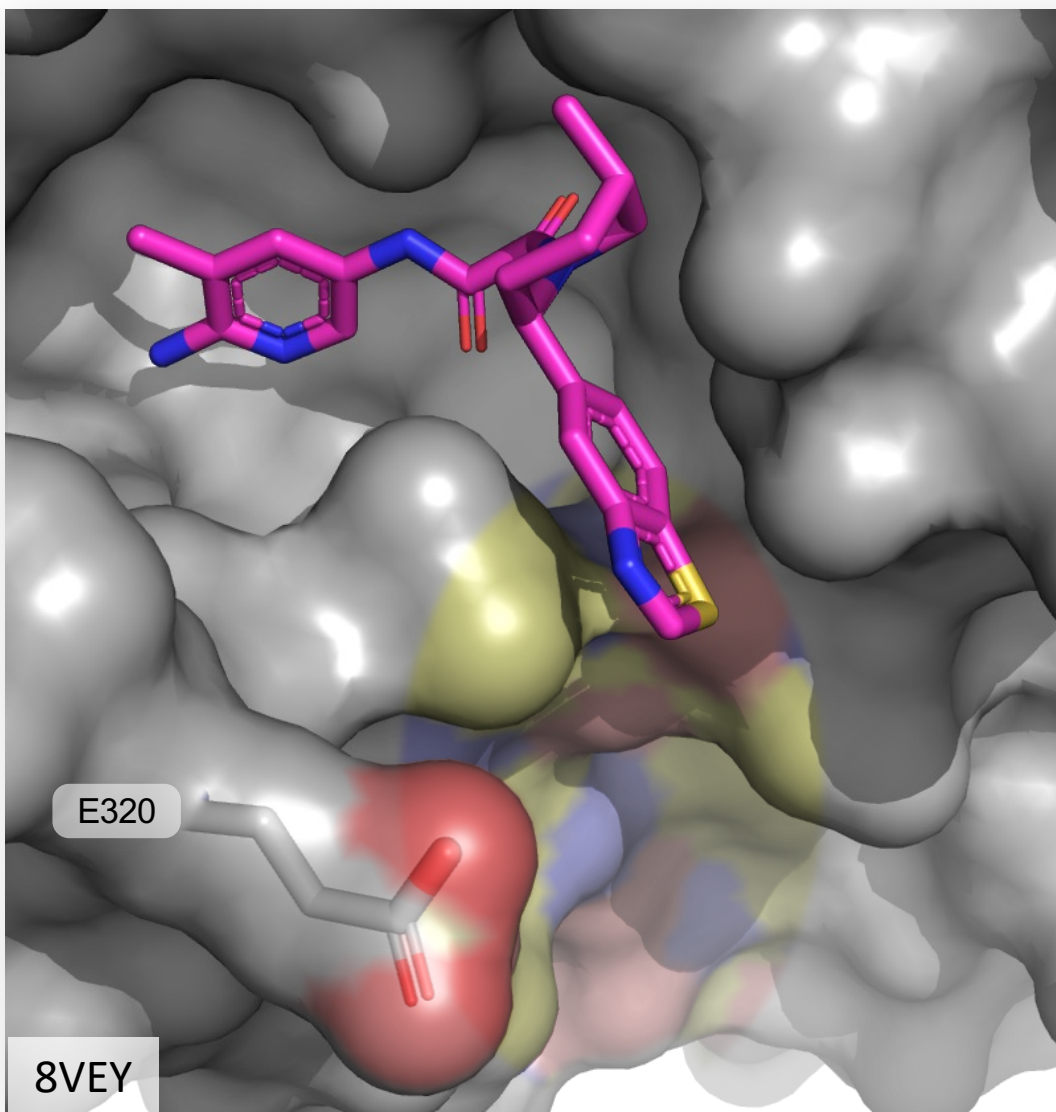
- Aminopyridine near MTA/SAM binding pocket, H-bonds to E435, E444, π -stacks with F327
- Oxamide NH and C=Os engaged in H-bonds
- Other favorable VdW interactions and polar interactions

Hypotheses to improve potency and selectivity:

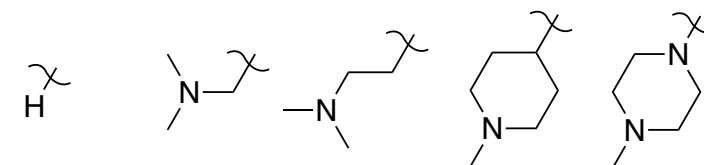
- A. MTA/SAM pocket
 - Reinforce E435 rotamer lock
- B. Benzothiazole region
 - Additional polar interactions
- C. Small pocket near piperidine

8VEY

Benzothiazole C2 substitution has broad impact on profile



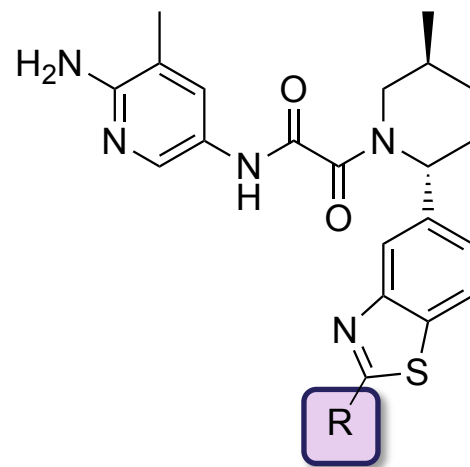
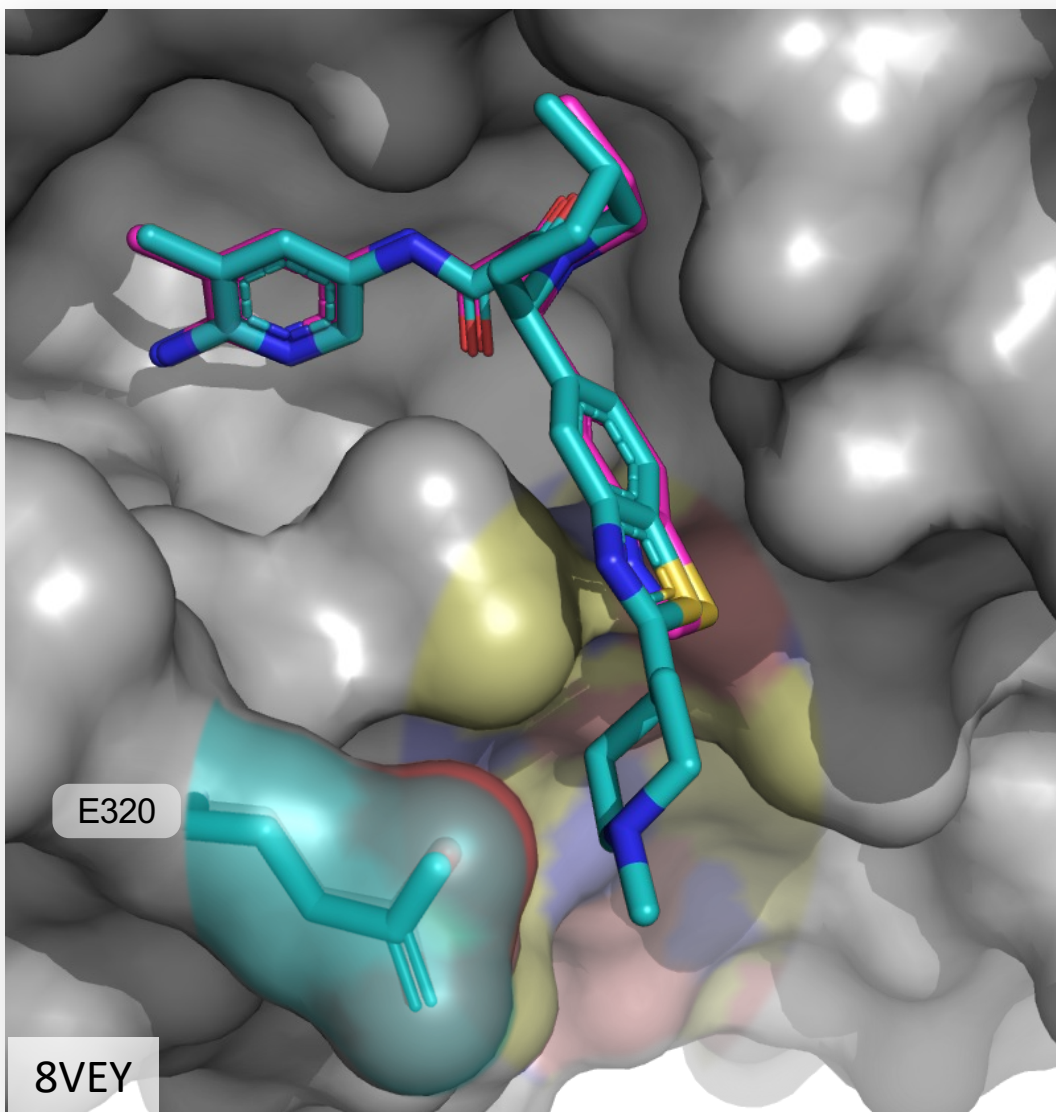
- Salt bridge with E320 gains up to 14-fold potency
- Selectivity largely unchanged
- Metabolic stability variable



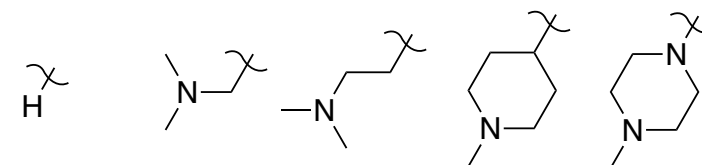
SDMA IC ₅₀ (μM)	0.009	0.01	0.01	0.001	0.004
Viability GI ₅₀ (μM)	0.10	0.03	0.02	0.007	0.027
Selectivity over MTAP WT GI ₅₀	15	11	7	8	10
hCl _{int} , mic (μL/min/mg)	14	30	10	10	57

TNG908

Benzothiazole C2 substitution has broad impact on profile



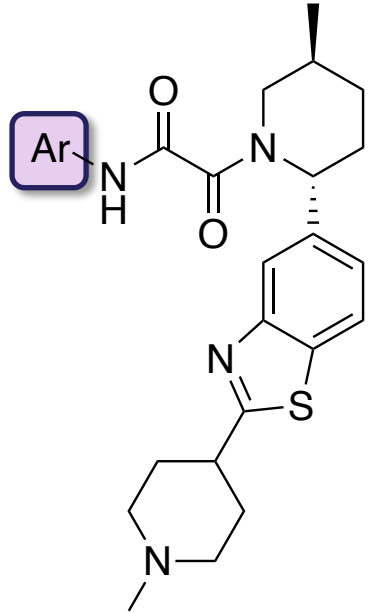
- Salt bridge with E320 gains up to 14-fold potency
- Selectivity largely unchanged
- Metabolic stability variable



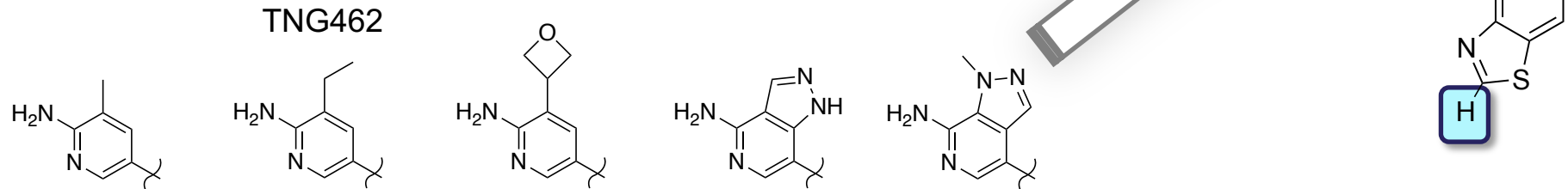
SDMA IC ₅₀ (μM)	0.009	0.01	0.01	0.001	0.004
Viability GI ₅₀ (μM)	0.10	0.03	0.02	0.007	0.027
Selectivity over MTAP WT GI ₅₀	15	11	7	8	10
hCl _{int} , mic (μL/min/mg)	14	30	10	10	57

TNG908

Non-additive SAR between ends of the molecules and unexpected selectivity modulation at benzothiazole C2

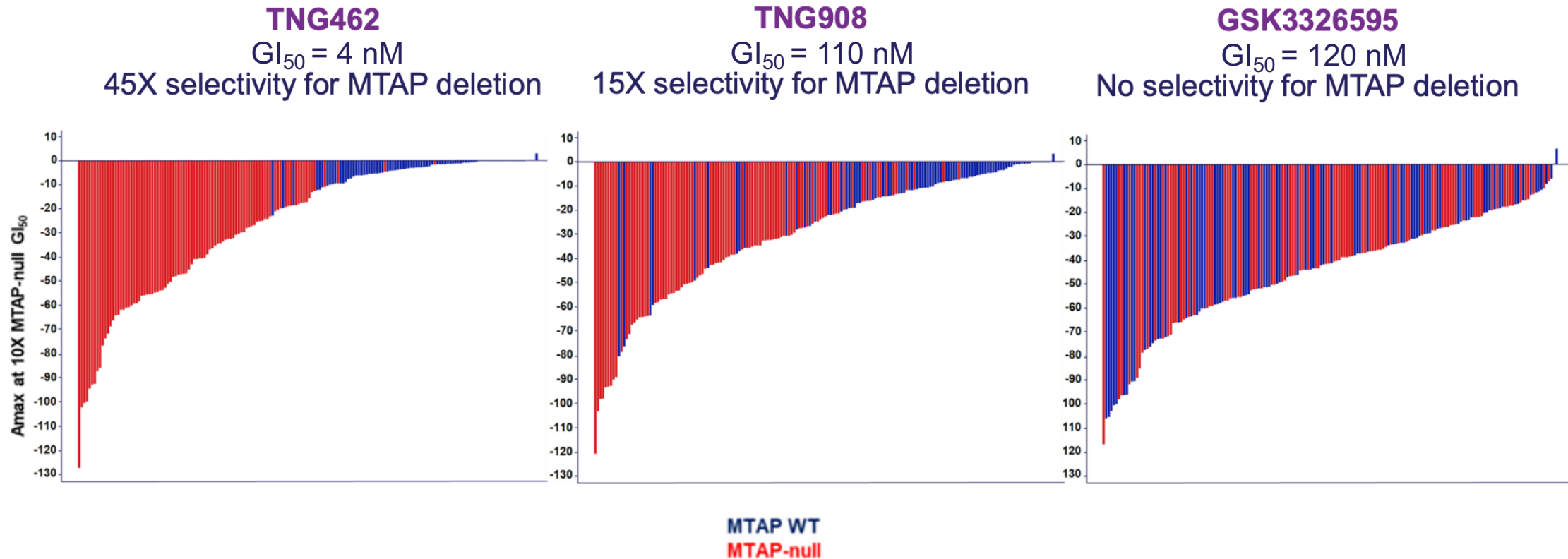


- Bicycles are potent but show reduced selectivity
- Piperidine rescues metabolic stability in previously unstable cases



SDMA IC ₅₀ (μM)	0.001	0.0008	0.002	0.001	0.001	0.002
Viability GI ₅₀ (μM)	0.007	0.004	0.007	0.002	0.004	0.01
Selectivity (to GI ₅₀ , WT)	8	30	24	6	8	40
hCl _{int} , mic (μL/min/mg)	10	15	< 10	18	15	24

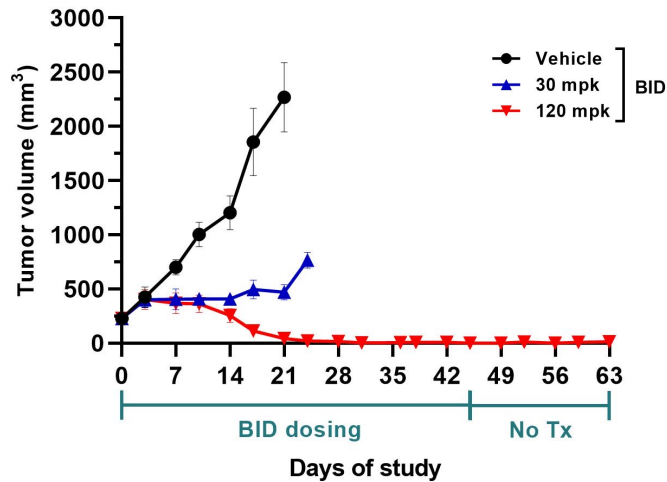
TNG908 and TNG462 are highly selective for MTAP deletion



- 180 cancer cell lines representing multiple cancer lineages including NSCLC, PDAC, bladder, CNS, and heme malignancies
- 7-day CellTiter-Glo assay
- Maximum effect at concentration equal to 10X HAP1 MTAP-null GI₅₀

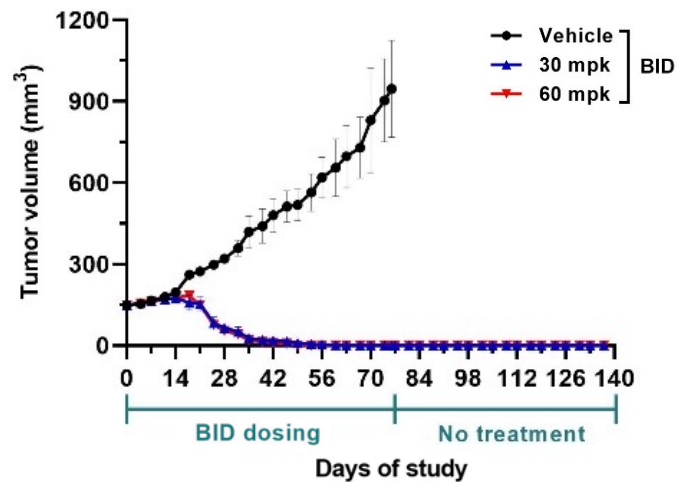
Strong, durable tumor regressions across histologies

TNG908 in MTAP-null Glioblastoma PDX



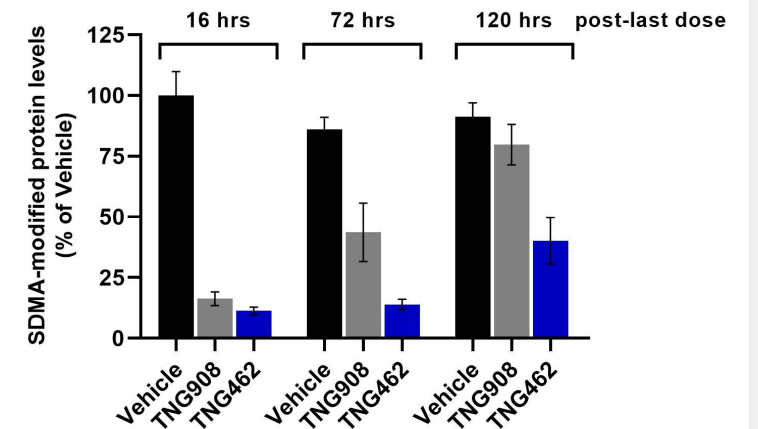
Sustained response after completion of dosing

TNG462 in MTAP-null NSCLC (squamous) PDX



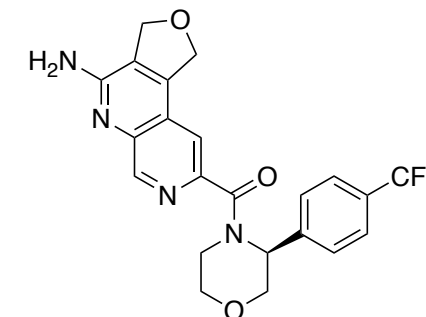
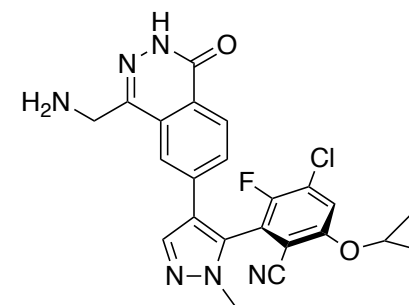
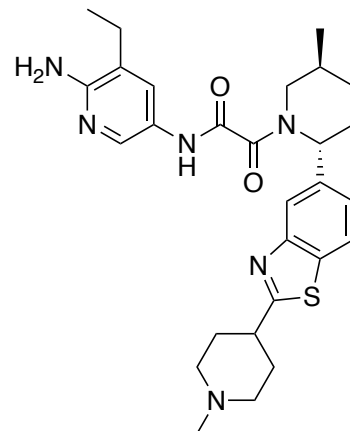
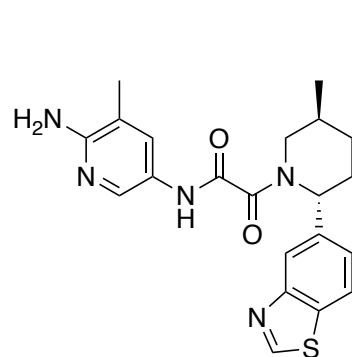
Sustained response after completion of dosing

TNG462 shows extended PD hold in vivo



LU99 CDX model
7-day PK/PD, 30mpk

Disclosed MTA-cooperative PRMT5 inhibitors in clinical trials



	TNG908	TNG462	MRTX1719	AMG 193
Company	Tango		Mirati / BMS	Amgen
Viability GI ₅₀ (nM)	110*	4*	8**	100**
Selectivity (to GI _{50, WT})	15*	45*	74**	40**
Hit finding approach (# molecules)	Peptide displacement HTS (~560,000)		SPR fragment (~3,000)	DEL (billions)

* HAP1

** HCT116, published data

Acknowledgements

John Maxwell
Kimberly Briggs
Doug Whittington
Haris Jahic
Matthew Tonini
Alan Huang
Janid Ali
Kenjie Amemiya
Charles Davis
Heather DiBenedetto
Stephene Ford
Sapna Makhija Garad
Shanzhong Gong
Deepali Gotur
Lina Gu
Colin Liang



Patrick McCarren
Dimitris Papoutsakis
Magnus Ronn
Alice Tsai
Erik Wilker
Hongling Yuan
Minjie Zhang
Wenhai Zhang



Oleg Michurin
Tatyana Galushka
Enamine Chemistry team



Wei Chen
Shuangyi Wan
WuXi Chemistry team

